ELSEVIER

Polymer 44 (2003) 2589–2597

polymer

www.elsevier.com/locate/polymer

Simulation of diffusion and relaxations of non-dilute star chains

Antonio Di Cecca, Juan J. Freire*

Departamento de Química Física, Facultad de Ciencias Químicas, Universidad, Complutense, 28040 Madrid, Spain

Received 30 September 2002; received in revised form 27 January 2003; accepted 27 January 2003

Abstract

Star polymer chains with 12 arms in a good solvent have been investigated using a dynamic Monte Carlo algorithm with the bond fluctuation model in the dilute, semidilute and concentrated regimes. We have characterized the self-diffusion coefficient and different relaxation modes of individual chains. We discuss the variation of the results with the arm length (or number of beads) and concentration. The ratio of diffusion coefficient of a star to that of a homologous linear chain is shown to increase progressively with concentration for overlapped non-entangled chains. It is also observed that diffusion and elastic relaxation of individual arms are more sensitive to the chains overlapping than global rotation or disentanglement between arms.

Keywords: Star chains; Bond fluctuation model; Monte Carlo dynamics

1. Introduction

Conformational properties of flexible star polymers [1] are significantly different to those of homologous linear chains because their topology has a great influence in local density. The specific mechanism for entanglement release and the impenetrability of the star cores are also important peculiarities reflected in the dynamics of non-dilute systems. Equilibrium and dynamic properties of star polymers have been characterized experimentally [2]. They have also been studied from the theoretical point of view, or with the help of computer simulations (Monte Carlo and Brownian Dynamics [1,3]). Currently, the behavior of single chains stars, together with the structure of semidilute systems, are reasonably well understood.

The dynamics of many-chain star systems have not received so much attention. Most theoretical studies on these systems have been focused on the mechanism of arm-retraction [4], in connection with the reptation theory, which is generally used to explain the dynamics of linear chains. The theory predicts an exponential decrease of the chain diffusion on chain length, which reproduces the experimental tracer diffusion of thee-arm stars in a matrix of linear chains [5]. The arm retraction is important, due to its direct influence on rheological and dielectric properties, and some refinements of the model [6–8] have successfully reproduce these properties. It is also found that the experimental self-diffusion of 3-arm chains in their melts, though also strongly dependent on chain length, is considerable faster than the tracer diffusion in linear chains [9], which reflects a more efficient reptation mechanism. On the other hand, self-diffusion of stars in non-dilute systems should be greatly influenced by the presence of impenetrable cores.

Simulation studies of non-dilute star systems are scarce. Explicitly dynamic algorithms are impractical for systems with a large number of units. Alternatively, performing dynamic Monte Carlo simulations of these systems with the simple cubic lattice model require the implementation of complex and specific bead jumps for the center of the star [10,11], in addition to the customary use of bents, crankshafts and end moves. Diffusion coefficients [12] and different relaxations [11] for non-dilute systems of stars with three and four arms have been obtained using this model. However, the bond fluctuation model [13] offers a considerably higher number of empty positions available around an occupied site and, furthermore, it only needs a single and simple form of elementary move, easier to generalize to any chain topology and more adequate to mimic stochastic bead jumps. The diffusion and relaxations of stars with three arms in dilute solution and a high polymer

* Corresponding author. Address: Departamento de Ciencias y Técnicas Fisicoquímicas, Universidad Nacional de Educación a Distancia (UNED), 28040 Madrid, Spain.

E-mail address: juan@hp720.quim.ucm.es (J.J. Freire).

0032-3861/03/$ - see front matter © 2003 Elsevier Science Ltd. All rights reserved.
doi:10.1016/S0032-3861(03)00114-9

volume fraction, $\Phi = 0.5$, equivalent to the melt, have been recently studied [14] using a variation of the bond fluctuation model [15]. Furthermore, we have previously shown that a slightly modified bond fluctuation model is adequate for the study of the structure of semidilute and concentrated solutions of many-arm star polymers [16] which, in the case of melts, has also been efficiently studied by means of the cooperative motion algorithm [17].

In the present work, we report diffusion coefficients and different relaxation modes for star chains of 12 arms characterized by dynamic Monte Carlo simulations with the bond fluctuation model at different concentrations, including single chain and volume fractions in the range $\Phi = 0.075-0.3$. This range corresponds to semidilute and concentrated solutions. The number of beads per arm ranges from 6 to 24. Therefore, we are not simulating fully entangled systems. We investigate the influence of the presence of relatively large neighboring cores on the dynamics behavior of the chains. We consider three types of relaxations: the elastic mode for individual arms, the rotational mode and the angular correlation between a pair of arms. We discuss the variation of the different properties with chain length and concentration, the relative mobility of stars with respect to homologous linear chains and the relative relationship between properties at different concentration regimes.

2. Computational description

The simulation model has been detailed in previous work, where we have implemented the bond fluctuation model [13] to investigate equilibrium and dynamic properties of different types of linear chains [18] and also to study the structure of non-dilute systems of self-avoiding walk 12-arm stars [16]. In the latter study, the only variation with respect to the original model consists in establishing a larger area of blocked (empty) sites around the central unit. Thus, the maximum distance between each central unit and its first neighbors is set as 4, while this maximum distance is maintained at the value of $\sqrt{10}$, proposed in the original model, for all the other beads. Without this modification, the center of the star would be trapped and could only oscillate around its initial position. Only providing this extra free space, we can achieve a long time displacement of the central units. Other beads are imposed to be at least at a distance of $2\sqrt{2}$ of the star center to avoid any arm crossing, though the density of neighboring units around the center is high enough to block any close approach of the remaining beads to the central point. We consider n self-avoiding walk molecules, each composed of a total of N beads divided into 12 arms, and a single-bead central unit, in a cubic lattice of length L, with periodic boundary conditions. The distance between adjacent sites, b, is taken as the length unit in the simulations. The value of L is chosen high enough to ensure that the number of interactions between different replicas of the same molecule is very small. ($L = 92-102$ in all our simulations.) The number of molecules is determined from the desired number of sites blocked by polymer beads, equivalent to the polymer volume fraction, $\Phi = 8nN/L^3$ (since, in our description [18], a bead actually blocks eight box sites). Elementary bead jumps are achieved just by randomly moving a bead to one of the closest six sites within its blocked cube. This way, the symmetric bead-jumps can effectively mimic the dynamic behavior of beads randomly interacting with their surrounding environment, reproducing the Rouse behavior for single chains and the crossover to a reptation-like behavior at high concentrations [13]. We start the dynamics using previously equilibrated samples [16]. These samples were obtained from initial conformations where the arms are placed in regular and parallel arrangements. Therefore, the samples are free from X-traps, which may affect chain dynamics in the long time regime [19]. The same dynamic algorithm can be employed to simulate star or linear dynamics, with the only extra provision of enforcing the bond connections of the different arms with the central unit in the star case. (This algorithm was also used in the equilibration of the star systems.)

The number of Monte Carlo steps used in the dynamic runs ranges between $(1-2)\times 10^6$ Monte Carlo steps. The Monte Carlo step constitutes the time unit in our simulations. All the results will implicitly be reported in units consistent with our length and time unit choices. Only a fraction of configurations, equal to 1/1000 of the total number of MC steps, is saved in the 'trajectory files'. These files contain the outbox coordinates which allow us to obtain diffusion coefficients. The relaxation modes are considerably faster and, therefore, we need a more compressed time scale. With this purpose, shorter trajectories were generated and saved every 5–150 Monte Carlo steps. For particular cases showing diffusion coefficient or relaxation times that noticeable deviate form the general behavior, according to our regression analysis, several independent trajectories are obtained.

Acceptance rates are small for the central bead (about 1×10^{-3} for single chains and 3×10^{-3} for $\Phi = 0.3$, depending weakly on N). These values, which are very probably dependent on the model details, are much smaller than the average acceptance rates. The latter values are 0.25–0.28 for single chains, and 0.21–0.22 for $\Phi = 0.3$, also weakly depending on N. This contrasts with a more significant variation with concentration for linear chains, 0.6 for $\Phi = 0.075$ and 0.27 for $\Phi = 0.3$, $N = 100$, also decreasing with N. Therefore, the central unit moves play an important role in the decrease of the average acceptance rate for our star model and this influence is more dramatic at low concentrations. Consequently, the mobility of the stars is conditioned by the motion of the central unit and other beads inside the star core for any value of concentration. This point will be discussed below in connection with the analysis of numerical results for the diffusion coefficient. We should remark, however, that the acceptance rate of the

central unit is in all cases significantly greater than the term $6D$, which characterizes the mean-square displacement of the stars. (Thus, the acceptance rate is about twice our $6D$ result for the case $\Phi = 0$, $N = 73$, which corresponds to the fastest diffusion). Therefore, the diffusion process is never controlled by the central unit moves, and it mainly depends on the collective motion of all beads.

3. Results

Overlapping concentrations, Φ^*, for the present star polymer systems were previously determined from the equilibrium sizes of single chains [16]. For the considered chains they are in the range $\Phi^* = 0.0270–0.0748$. Therefore, some degree of overlapping is present in all our non-dilute systems; the stars with shorter arms are close to overlapping concentration at $\Phi = 0.075$. The equilibrium collective scattering data of the systems with $\Phi = 0.3$ show a near-to-flat variation with the wavevector indicating that these systems correspond to concentrated solutions [16].

We have determined the diffusion coefficients by analyzing the linear correlation of the mean-square displacement of the center of masses vs time for individual chains in the trajectory files, see Fig. 1, where a good linear correlation is found in a wide interval of time values. In Table 1, we show the results for different arm lengths and concentrations. Uncertainties were estimated according to the deviations found for different adequate choices of the interval fitting, and also to the differences observed for results in the cases where independent runs are performed. The relative errors for the values contained in Table 1 are in the range 5–10%. For the discussion of these data, we will sometimes refer to the simulation values of diffusion coefficients corresponding to linear chains (same model)

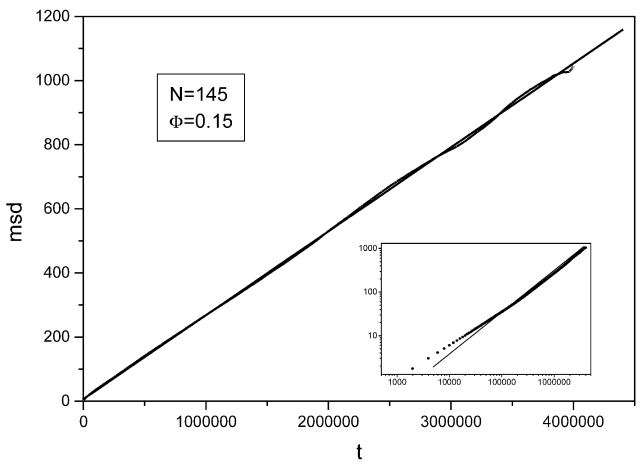

Fig. 1. Mean-square displacement of the center of masses (msd) vs t for a 12-arm star. The simulation data are represented by (overlapped) open circles. The linear fit from which the diffusion coefficient is extracted is shown as a solid line. The log–log plot of the simulation data, and their fit to a linear function with a slope close to 1 (solid line) is shown in the inset. For this case [16], $\langle R_C^2 \rangle = 184$.

Table 1
Diffusion coefficients of 12-arm stars

Φ	$D \times 10^4$			
	$N = 73$	$N = 109$	$N = 145$	$N = 289$
0	1.83	1.33	0.99	0.50
0.075	0.97	0.61	0.45	0.22
0.15	0.59	0.47	0.43	0.23
0.30	0.51	0.42	0.38	0.20

reported in our previous work [18]. It is interesting to note that the single chain results for the diffusion coefficients of our stars are considerably smaller than for the homologous linear chains with the same total number of units. We have also observed a similar though smaller effect in previous simulation data obtained for stars of 3 and 4 arms with a simple lattice model [20]. The decrease of mobility in the stars is due to the accumulation of units near the center. A single linear chain has a similar density of beads along the chain contour. Therefore, the friction suffered by all units is equivalent and small. However, the friction around the center is much higher than in the outer part of a star in dilute solution and, therefore, the central unit moves, crucial to the displacement of the molecule, are severely inherit. The effect is directly related with the model details and, therefore, it is model dependent at least in some extension. (In the present version of the bond fluctuation model, the choice of the maximal distance between the central unit and its first neighbors may substantially change the star mobility.)

It should be considered, however, that this explanation is only valid for free-draining chains, consistent with the dynamic Monte Carlo algorithm that we are using in the simulations. In fact, log–log plots of D vs. N for $\Phi = 0$ and for 0.075 show good linear correlations with slopes close to -1, in good agreement with the theory for free-draining chains. If hydrodynamic interactions are included, however, the equilibrium distribution of beads within the molecule is the main factor to determine its mobility. Actually, the chains behave as equivalent compact spheres, with D inversely proportional to the hydrodynamic radius. Therefore, the more compact star chains are predicted to diffuse faster than their homologous linear chains. Hydrodynamic interactions are predominant in dilute solutions and, therefore, our data for single chains cannot explain these systems. The experimental ratios between diffusion coefficients of linear and star chains, D_{lin}/D_{star} in dilute solutions are smaller than the unity and have been adequately reproduced through alternative simulations where hydrodynamic interactions are explicitly taken into account [3]. In any case, it should be considered that hydrodynamic interactions are progressively screened out in non-dilute systems [21], and, therefore, the present dynamic Monte Carlo data should give a more consistent description of non-dilute systems, where hydrodynamic interactions are partially or totally

suppressed. According to this explanation and the model dependent features discussed in the preceding paragraph, the present results for free-draining single chains are only relevant as a reference to understand the rest of our simulation data and should not be compared with experimental data.

According to the data shown in Table 1, the variation of D with concentration is significant in the concentration range between dilute solution and overlapping concentration. A comparison with the simulation results for diffusion coefficients obtained for linear chains of similar number of units [14] and similar Φ, reveals that the variation in this concentration range is greater for the stars. The enhanced decrease with concentration for the stars is obtained even though, as discussed in the previous paragraph, the diffusion coefficients for free-draining single stars are smaller than for linear chains in the absence of hydrodynamic interactions. Some recent experimental data [22] based on NMR show a sharp decrease of D with Φ for concentrations close to Φ^*. Although we have not attempted a detailed characterization of this region, our simulation data also seem to follow this trend. However, the variation with concentration of our D values is small for concentrated solutions.

At overlapping concentration the chains suffer an important loss of mobility since the systems adopt an 'ordered structure' with the star cores placed at convenient mean distances [1]. This ordering is characterized by a peak in the scattering function, which was detected in our previous analysis of the equilibrium data for these systems [16]. The diffusion of stars between these ordered cores may become difficult. For more concentrated systems, the increase of local friction affects mainly to the external part of the chains and, according to the data, it apparently does not lead to an important reduction of diffusion mobility, maybe because the core behavior mainly determines the dynamics of these short-arm stars. However, the latter conclusion can be taken with some caution, since it may not be valid for chains with longer arms that are fully entangled with arms belonging to neighboring chains. Considering fully entangled chains, a higher concentration would imply an important reduction of the tube width, affecting the star mobility through the arm retraction mechanism. It seems that both factors, arm retraction and diffusion through the core obstacles, may be similarly important for some systems. The predominance of each one depends on the extension of the relative extension of the regions affected by the core exclusion and the regions occupied by the partially or totally entangled external parts of the arms in each particular system. Accordingly, the influence of concentration on the self-diffusion of star chains is very different than in the case of linear chains, where a more monotonous change is observed.

This is clearly observed in Fig. 2. In the inset, we show the diffusion coefficients of the overlapped stars vs the reduced concentration, Φ/Φ^*. A noticeable change of

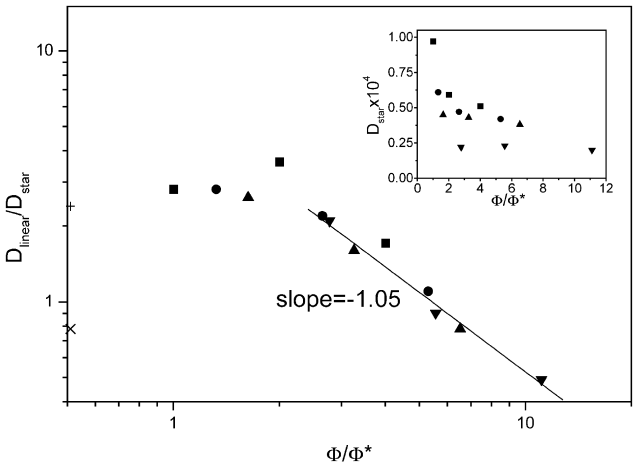

Fig. 2. D_{lin}/D_{star} vs Φ/Φ^* for different values of N and Φ. $N = 73$, squares; $N = 109$, circles; $N = 145$, up triangles; $N = 289$, down triangles; single chain value obtained for $N = 109–289$, (+); single chain value calculated with hydrodynamic interactions [3], (×). (The single chain data are indicated at an arbitrarily chosen low-concentration.) Solid lines, linear fit for the $\Phi \gg \Phi^*$ data. Inset: D_{star} vs Φ/Φ^*, same notation for different values of N.

behavior is observed between the strong concentration dependence of the shortest chains, low Φ/Φ^*, and the much weaker variation for longer chains. Also, we have plotted in the main part of Fig. 2 the ratio D_{lin}/D_{star} vs Φ/Φ^*, where we combined the diffusion coefficient data obtained from our simulations of star systems, together with interpolations or extrapolations for the homologous linear chains at the same concentrations. The latter values are calculated from fitting equations [18] that describe the variation with N for linear chains at a given concentration in the range 40–100. (The extrapolations for $N = 289$ may, therefore, represent a slight overestimation of D_{lin}, since the dependence with N is more pronounced for longer chains, which are closer to exhibit full entanglements.) The results corresponding to different number of units and concentrations seem to follow a universal behavior. The ratios at high Φ show a monotonous decrease with the degree of overlapping. However, the data for $\Phi/\Phi^* < 2$ (including the single chain ratio, practically constant for $N = 109–289$ and shown in Fig. 2) are more compatible with an initial increase, which is consistent with the loss of mobility of the stars at overlapping concentrations. This initial trend is remarked when we consider the effect of hydrodynamic interactions at dilute solutions for real samples of non-draining chains. Thus, the ratio for D_{lin}/D_{star} corresponding to long single chains with hydrodynamic interactions [3] (also included in Fig. 2) is smaller than our simulation results except for $\Phi/\Phi^* > 7$, while hydrodynamic effects are expected to be fully screened out before reaching this high degree of overlapping. Therefore, our simulation data for the overlapped systems should give an adequate representation of real systems for concentrations smaller than $\Phi/\Phi^* > 7$. Consequently, real chains with hydrodynamic interactions, i.e. with a smaller value of D_{lin}/D_{star} at

low concentration, should exhibit a sharper intermediate maximum for this ratio than our free-draining simulation systems. For $\Phi/\Phi^* > 2$ the data apparently follow a $D_{lin}/D_{star} \approx (\Phi/\Phi^*)^x$ power-law dependence with a purely empirical exponent value of $x \cong -1$. This behavior reflects the strong increase of mobility in the stars due to their smaller size, with respect to their homologous linear chains. The feature cannot be balanced by the restrictions due to topology effects in the present simulation systems, where branches are far to be fully entangled.

It is also interesting to compare the self-diffusion of stars with linear chains composed of fewer units but with a similar arm extension. With this purpose, we consider the 'chain span', N_{sp}, as the number of units of two arms in a star, or the total number of units in a linear chain [14]. (The further increase of arm lengths due to core effects somehow distort the realtionship between N_{sp} and the star size for the present case of a star with many branches. However it still may still be used for a qualitative comparison of the behavior of linear and star chains.) In Fig. 3, we represent D vs N_{sp} for the 12-arm stars at our highest concentration and compare the results with the data for linear chains at the same concentration. Our discussion takes also in consideration the results included in Fig. 7 of Ref. [14], obtained for stars of 3 arms (represented with a variation of the bond fluctuation model) in the melt (actual volume fraction $\Phi = 0.5$). It is observed that the 12-arm stars have much smaller mobility than the linear chains with same N_{sp}. The decrease in D is more remarkable than for the 3 arm stars.

The differences in the linear and star chain mobility behavior at high concentration are not only due to size effects, as it is shown in Fig. 4, where D is plotted vs the quadratic radius of gyration, $\langle S^2 \rangle$. In the inset of the figure, it is observed that the data for linear chains show a monotonous behavior at any concentration, though the systems with higher Φ show a strongest decrase for the

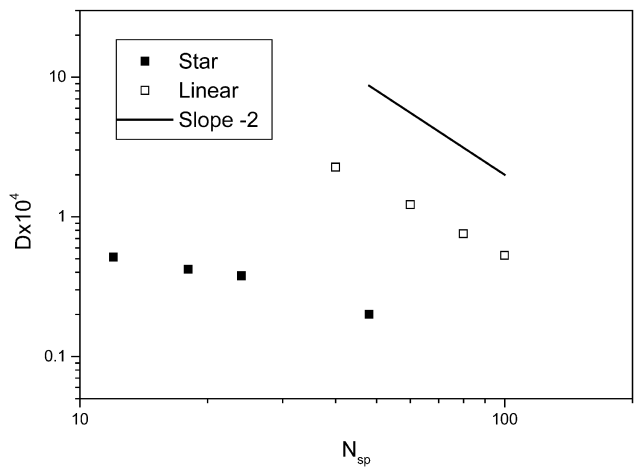

Fig. 3. Comparison between the simulation data of the translational diffusion for linear [18] and 12-arm star chains at $\Phi = 0.3$ vs their respective N_{sp}. The solid line is the slope according to the reptation theory for linear chains.

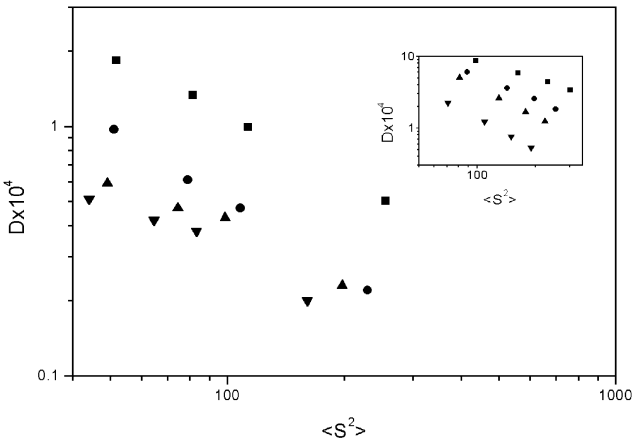

Fig. 4. D vs $\langle S^2 \rangle$ for star chains at different concentrations. $\Phi = 0$, squares; $\Phi = 0.0075$, circles; $\Phi = 0.015$, up triangles; $\Phi = 0.3$, down triangles. Inset: similar data for linear chain (same notation).

longer chains, marking the onset of entaglement effects. However, the aspect of the data for the more concentrated star systems is more irregular, showing a range where mobility does not decrease as significantly as expected for larger sizes.

It is verified that the 12-arm stars at high concentration have a slow variation with N_{sp} in this chain length region, which can be easily appreciated in Fig. 3. This variation is, in fact, slower than the Rouse result $D \approx N^{-1}$ obtained for the dilute systems. In fact, it is close to a $D \approx N^{-1/2}$ dependence, both for $\Phi = 0.15$ and 0.3. The latter proportionality implies diffusion coefficients inversely proportional to the chain sizes (excluded volume effects, as well as hydrodynamic interactions, are mainly screened out at these concentrations). The result is consistent with the Stokes law, and, therefore, the non-dilute small stars essentially diffuse as hard-sphere cores. This fact confirms that the dynamics of non-dilute stars with short non-entangled arms is very similar to that of simple liquids composed of rigid molecules. However, the most concentrated systems exhibit an important log–log curvature for the largest chains, not shown by the linear chains.

Nevertheless, the decrease of diffusion coefficients with the chain size is still smaller than the dependence on N obtained for linear chains at the same concentrations, even for our highest values of N_{sp}. It should be considered that the values of N_{sp} are always small and cannot be substantially increased for the 12-arm chains without dealing with an inconveniently high total number of beads. Furthermore, for the considered range of values of N_{sp}, the linear chains have not reached the expected $D \approx N^{-2}$ dependence corresponding to fully entangled systems. The analysis of the simulation data reported and discussed in Ref. [14] for 3-arm stars in the melt (with a similar range of values of N but 4 times higher values of N_{sp}) showed a close to linear log–log behavior, consistent with $D \approx N^{-2.2}$, also compatible with the theoretically predicted exponential dependence [4], which suggests an important arm retraction effect. It should

be mentioned that a shorter entanglement chain length in the melt, at about $N = 40$, is associated with this modified version of the bond fluctuation model [14,15], which may also explain the earlier exhibition of this effect. We conclude again that the influence of intermolecular entanglements is not fully manifested in our systems, but it may be important for longer branches. Real samples of many-arm stars may, however, exhibit only a partial degree of entanglements, except for large molecular weights, and the self-diffusion in some non-dilute systems or melts may show a behavior intermediate between the predictions for a system of hard spheres and for a system of fully entangled chains relaxing through the modified arm-retraction mechanism.

The different degree of entanglement of linear chains and branches, together with the steric effects of the star cores can justify the qualitative behavior shown by the simulation data in Fig. 2, in terms of exponent x. Thus, the diffusion coefficient of moderately long linear chains at high concentration can be expressed by $D \approx N_{\text{lin}}^{-(x_D)}$, where $(x_D)_{\text{lin}}$ is a value between 1 and 2. The homologous star chains with many branches at high concentration, however, are mainly affected by the steric effects due to the impenetrability of cores and, therefore, $D \approx N_{\text{star}}^{-(x_D)}$, with a smaller exponent $(x_D)_{\text{star}} \geq 1/2$. (A constant $(x_D)_{\text{star}}$ implies considering a relatively narrow range of N.) Therefore, $\Delta x_D = (x_D)_{\text{lin}} - (x_D)_{\text{star}} > 0$. (However, Δx_D would be negative for fully entangled long branches where modified arm retraction is the predominant effect.) The linear and star chains should follow the same dependence of D vs N at dilute solution, i.e. below overlapping concentration. On the other hand, the length dependence of Φ^* with N in terms of exponent ν, corresponding to scaling law of the radius of gyration in dilute solution, $\langle S^2 \rangle^{1/2} \approx N^{\nu}$, is $\Phi^* \approx N^{(1-3\nu)}$. Consequently, in the semidilute regime, exponent x can only link the predictions for dilute and concentrated conditions if it is expressed as

$$x = \Delta x_D/(1 - 3\nu) \tag{1}$$

Considering the results obtained in our previous simulations for the diffusion coefficients of linear chains [18] and the present data for stars we get, $\Delta x_D \approx 0.9$ for $\Phi = 0.3$. This result together with $\nu \approx 0.6$ gives $x \approx -1.1$. Assuming that the linear chains are completely entangled, and the stars behave as cores with unentangled branches, i.e. using Eq. >(1) with the theoretical values $\Delta x_D = 3/2$ and $\nu = 0.589$, we get $x = -1.96$. If the linear chains are also unentangled, i.e. taking $\Delta x_D = 1/2$ and $\nu = 0.589$, we obtain $x = -0.65$.

We have also obtained results for different relaxation modes of the stars. In particular, we have investigated the elastic relaxation of arms, defined as

$$C_e(t) = \frac{\langle R_C(\tau) R_C(\tau + t) \rangle_\tau - \langle R_C \rangle^2}{\langle R_C^2 \rangle - \langle R_C \rangle^2} \tag{2}$$

where $R_C(t)$ corresponds to the center-to-end vector of individual branches at time t. This vector can easily we evaluated from the saved trajectory file. The final results for $C_e(t)$ are averaged over all arms and also over a sample of all molecules contained in the system. These results are fitted to a single exponential in a wide interval of values of t. The fitted exponent allow us to estimate the corresponding relaxation time, τ_e. An initial curvature from the exponential behavior is apparent for some systems. This curvature becomes wider as concentration increases. This effect significantly reduces the accuracy of our τ_e values.

The results for τ_e are contained in Table 2. Uncertainties are estimated as in the case of the diffusion coefficient. Relative errors for relaxation times are 10–20%. It can be observed that the relaxation times have a pronounced increase with N at any concentration. Log–log plots of τ_e vs N yield slopes ranging from 2.4 to 2.6. The theoretical prediction for single chains is [1] $\tau_e \approx N^{1+2\nu}$. Our previous results for single stars with 3 and 4 arms (simple cubic lattice model) yielded exponents 2.17 and 1.94 close to the theoretical $1 + 2\nu$, with $\nu = 0.589$, and in agreement with other simulations for single 3-arm stars [14,23,24] which gave values in the range 2.2–2.3. The slightly higher current value of 2.4 for the exponent in the case of single chains may reflect a partial degree of intramolecular entanglements between arms in the core region of many-arm chains. Brownian dynamic studies [25,26] of single many-arm star chains have also investigated τ_e, though the analysis of results have been mainly focused to confirm the weak dependence on the number of arms, also predicted by the theory. However, we should mention that the numerical

Table 2
Different relaxation times of 12-arm stars. The fitted exponents y for their specific power-law dependencies $\tau_i \approx N^y$ are also shown for each concentration

Φ	N	$\tau_e \times 10^{-3}$	$\tau_r \times 10^{-4}$	$\tau_a \times 10^{-4}$
0	73	0.24	0.56	0.25
	109	0.51	1.2	0.35
	145	1.2	2.5	0.77
	289	6.3	8.9	3.0
y		2.4	2.03	1.93
0.075	73	0.24	0.6	0.3
	109	0.8	1.4	0.54
	145	1.6	2.6	0.93
	289	10	11	3.7
y		2.57	2.03	1.85
0.15	73	0.3	0.8	0.3
	109	0.9	1.5	0.5
	145	1.8	2.5	0.8
	289	9.5	10	3.6
y		2.51	1.86	1.86
0.30	73	0.59	0.8	0.4
	109	1.5	1.87	0.6
	145	3.3	3.0	1.3
	289	18	10.6	5.2
y		2.51	1.86	1.89

results reported in Table 2 of Ref. [25] for stars of 10 arms with $N = 50$ and 100 (i.e. also with a small number of beads per arms) show a variation with N smaller and slightly closer to the theoretical prediction that the present results (apparent exponent of ca. 2).

The results for higher concentrations show greater exponents in the range of 2.5–2.6. An important increase of the exponent with respect to the single chain case has been reported for 3-arm stars in the melt [14]. It seems that this relaxation is remarkably sensitive to the progressive increase of the branch entanglements due to chain overlapping, since this is the main effect expected from the increase of chain concentration. However, the variation with concentration is small in the range $\Phi = 0.075–0.15$. This feature is also observed for the other relaxation processes that will be described below. Apparently, once the star cores are ordered beyond overlapping concentration, the relaxations are not affected by a moderate increase of the bead density in the outer regions. However, in the particular case of the elastic mode, an abrupt increase of the relaxation times is observed at $\Phi = 0.3$, where density becomes more uniform in all the regions. The relaxation mechanism for the elastic mode is particularly affected by the friction of more internal parts of the star, and it seems to be very sensitive to this effect when the systems reach the concentrated regime.

We have also studied the rotational relaxation, described by the function

$$C_r(t) = \frac{\langle \mathbf{R}_C(\tau)\cdot\mathbf{R}_C(\tau+t)\rangle_\tau}{\langle R_C^2\rangle} \tag{3}$$

This relaxation is considerably slower than the elastic mode and, therefore, it is difficult to investigate with explicitly dynamic algorithms, which can only cover relatively short times [1]. As shown in Fig. 5, our results again exhibit an exponential behavior in a wide interval of values of time (after an initial curvature) from which we determine the rotational relaxation time, τ_r, also contained in Table 2. The

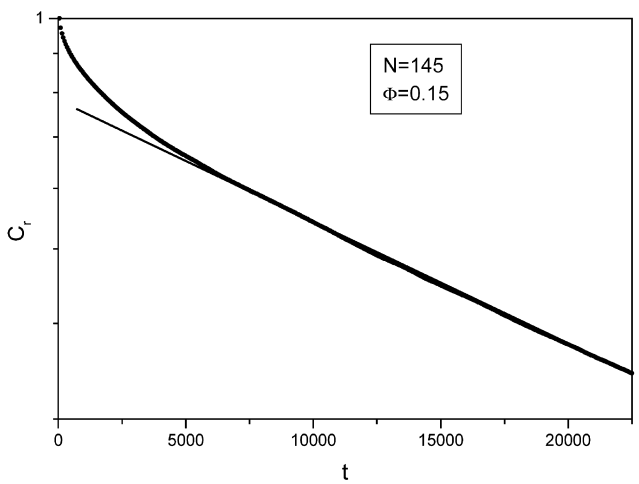

Fig. 5. Simulation data for $C_r(t)$ overlapped circles, fitted to an exponential function (solid line).

expected variation of τ_r with N for single chains can also be expressed in terms of a power law $\tau_r \approx N^{1+2\nu}$. The results for the exponent are close to the theory for all concentrations (it should be considered that $\nu = 1/2$ in the melt, since the excluded volume effects are screened out). The variation with concentration is moderate in the whole range of volume fractions. Consequently, it seems that the reorientation of the star is less affected than expected by the increase of friction or by the entanglements in the outer part of the stars, at least for the present non-fully entangled systems.

Another interesting relaxation mode describes the loss of angular correlation between two arms, i and j. This effect can be quantified by means of the function

$$C_a(t) = \left[\frac{1}{f(f-1)}\right] \sum_i \sum_{j\neq} \langle[\mathbf{R}_C^i(\tau)\cdot\mathbf{R}_C^j(\tau)][\mathbf{R}_C^i(\tau + t)\cdot\mathbf{R}_C^j(\tau+t)]\rangle_\tau, \quad i \neq j \tag{4}$$

which can also computed from the trajectory file (averaging over a sample of molecules and over a selection of pairs of arms with large initial correlations). The function also decay exponentially in a wide interval, from which we obtain the relaxation time, τ_a, whose estimations are included in Table 3. These values are considerably greater than the corresponding results for τ_e, but smaller than the rotation relaxation times. In Fig. 6, we compare the elastic and rotation relaxations with the decay of an adequately normalized function $C_a(t)$. Apparently, the two arms loose their alignment before any of them is totally reoriented, unless the arms are strongly entangled. Moreover, the variation of τ_a with N or the concentration follows similar trends that the variation observed for the rotational time, i.e.

Table 3
Values of the parameter $\langle R_C^2\rangle/D\tau_r$

Φ	N	$\langle R_C^2\rangle/D\tau_r$
0.0	73	92
	109	95
	145	89
	289	114
0.075	73	158
	109	173
	145	174
	289	182
0.15	73	186
	109	194
	145	172
	289	164
0.30	73	156
	109	150
	145	135
	289	143

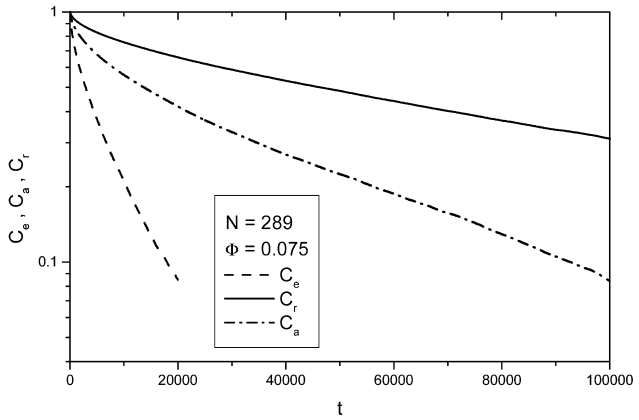

Fig. 6. Comparision between different relaxation processes for a 12-arm star.

the results are not very sensitive to the increase of friction or intermolecular entanglements in the external part of the star.

The main Rouse relaxation time, τ_1, is correlated with the translational diffusion coefficient in the case of linear chains, since both quantities are similarly sensitive to friction. These quantities can actually be combined together with the mean-square end-to-end distance in the parameter $\langle R^2\rangle/D\tau_1$. This parameter shows a small variation with chain length and concentration, according to our previous data for non-diluted self-avoiding linear chains [12,18], being always close to the value predicted by the Rouse theory [27], $3\pi^2$. In the case of stars, it seems adequate to correlate the rotational time and the diffusion coefficient [1]. Therefore we define the parameter $\langle R_C^2\rangle/D\tau_r$, where we have substituted the mean square end-to-end distance in linear chains by the mean-square center-to-end distance of the arms for the case of stars. (Values of $\langle R_C^2\rangle$ for the present systems were reported earlier [16].) The results are shown in Table 3. For single chains, it can be observed that our values of $\langle R_C^2\rangle/D\tau_r$ are about three times higher than the Rouse theory value, and they suffer an increase for non-dilute systems. Our previous simulations for stars of 3 and 4 arms were, however, more compatible with the value $3\pi^2$ for the different concentrations [12].

A constant value of $\langle R_C^2\rangle/D\tau_r$ for chains of different forms at different volume fractions would imply that the frictional effects of changing topology and concentration are similar for D and τ_r. This does not seem to be the case when we compare the linear chains and the 12-arm stars. We have discussed that our single chain 12-arm stars exhibit diffusion coefficient that are significantly smaller than those of linear chain, due to the high friction in the star core, which slows down the crucial moves of the star center. However, the star rotation is not affected by this problem, since the arms can be efficiently be reoriented by changing its more external parts. In fact, the observed increase in parameter $\langle R_C^2\rangle/D\tau_r$ with respect to the Rouse prediction is similar to the decrease of the diffusion coefficient with respect to its value for a homologous linear chain. As previously discussed, the decrease of the star mobility due to restrictions in the junction point may be greatly conditioned by the model details. At higher concentrations, close to overlapping conditions, core ordering affects mainly to the diffusion coefficient, but not so much to rotation, explaining the further increase of $\langle R_C^2\rangle/D\tau_r$. It should be remarked that this tendency does not have to be influenced by the model characteristics. Finally, at the highest concentrations, the diffusion coefficients only suffer a modest increase and the values of $\langle R_C^2\rangle/D\tau_r$ tend to be closer to the results obtained for single chains. In all cases, $\langle R_C^2\rangle/D\tau_r$ does not systematically vary with N at any given concentration. (Fluctuations can easily reach 20% since this parameter combines three simulation results, two of them indirectly obtained through fitting procedures.) We should mention that an increase of $\langle R^2\rangle/D\tau_1$ with respect to the theory value was also observed in the case of linear chains in the theta region [18]. As in the present case, this increase for theta systems was associated to a restriction of mobility and seems to be mainly caused by the decrease of the diffusion coefficient.

Although the present simulations cannot mimic the behavior of fully entangled chains, our data show other specific features of the diffusion and relaxations of many-arm stars in non-dilute systems. The stars exhibit variations of their dynamic properties with arm length (or total number of beads) and concentration considerably more complex than the homologous linear chains. Entangled branches may reduce drastically the star mobility. However, in the chain length range covered by the simulations, the influence of entanglement is much lighter than in the case of the homologous linear chains and the mobility of stars relative to the linear chains actually increases with concentration in the semidilute regime. In the region close to overlapping concentration, the main feature in the dynamic is the impenetrability of the star cores. Relaxations do not seem to be much affected by the increase of friction in the outer part of the chains, which is again manifesting the small influence of branch entanglements in this simulation data.

Acknowledgements

This work has been supported by the European TMR Research network ‘NEWRUP’ and Grant BQU2002-04626-C02-02 of the DGI (MCYT, Spain).

References

[1] Grest GS, Fetters LJ, Huang JS, Richter D. Adv Chem Phys 1996;94:67.
[2] Burchard W. Adv Polym Sci 1999;143:133.
[3] Freire JJ. Adv Polym Sci 1999;143:35.
[4] Brochard-Wyart F, Ajdari A, Leibler L, Rubinstein M, Viovy JL. Macromolecules 1994;27:803.
[5] Shull KR, Kramer EJ, Fetters LJ. Nature 1990;345:790.
[6] McLeish TCB, Milner ST. Adv Polym Sci 1999;143:195.

[7] Milner ST, McLeish TCB. Macromolecules 1998;31:7479.
[8] Watanabe H, Matsumiya Y, Inoue T. Macromolecules 2002;35:2339.
[9] Bartels CR, Crist B, Fetters LJ, Graessley WW. Macromolecules 1986;19:785.
[10] Sikorski A. Makromol Chem Theor Simul 1993;2:309.
[11] Molina LA, Freire JJ. Macromolecules 1999;32:499.
[12] Freire JJ, Molina LA, Rey A, Adachi K. Macromol Theor Simul 1999; 8:321.
[13] Binder K. In: Binder K, editor. Monte Carlo and molecular dynamics simulations in polymer. New York: Oxford University; 1995. Chapter 1.
[14] Brown S, Szamel G. Macromol Theor Simul 2000;9:14.
[15] Shaffer JS. J Chem Phys 1995;103:761.
[16] Di Cecca A, Freire JJ. Macromolecules 2002;35:2851.
[17] Pakula T, Vlassopoulos D, Fytas G, Roovers J. Macromolecules 1998; 31:8931.
[18] Rubio AM, Storey M, Lodge JFM, Freire JJ. Macromol Theor Simul 2002;11:171.
[19] Tanaka M, Iwata K, Kuzuu N. Comput Theor Polym Sci 2000; 10:299.
[20] Molina LA. PhD Thesis, Universidad Complutense de Madrid; 1998.
[21] Doi M, Edwards SF. The theory of polymer dynamics. Oxford: Clarendon Press; 1986.
[22] Fleischer G, Fytas G, Vlassopoulos D, Roovers J, Hadjichristidis N. Physica A 2000;280:266.
[23] Sikorski A, Romiskowski PJ. Chem Phys 1996;104:8703.
[24] Xu G, Mattice WL. Macromol Theor Simul 2002;11:649.
[25] Grest GS, Kremer K, Witten TA. Macromolecules 1987;20:1376.
[26] Grest GS. Macromolecules 1994;34:3493.
[27] Doi M. Polym J 1973;5:288.